Numerical irreversibility in self-gravitating small N-body systems

Numerical irreversibility in self-gravitating small N-body systems

Nobuyoshi Komatsu [a], Takahiro Kiwata [a] and Shigeo Kimura [b]

[a] *Department of Mechanical Systems Engineering, Kanazawa University*

[b] *The Institute of Nature and Environmental Technology, Kanazawa University, Kakuma-machi, Kanazawa, Ishikawa 920-1192, Japan*

Abstract

Numerical irreversibility due to round-off errors appearing in self-gravitating N-body systems is investigated by means of molecular dynamics methods. As a typical self-gravitating system, a closed spherical system consisting of N point-particles, which are interacting through the Plummer softened potential, is considered. In order to examine the numerical irreversibility, time-reversible simulations are executed: that is, a velocity inversion technique for a time-reversal operation is applied at a certain time during the evolution of the system. Through the simulations with various energy states, it is found that, under a restriction of constant initial potential energy, numerical irreversibility prevails more rapidly with decreasing initial kinetic energy. In other words, the lower the initial kinetic energy (or the lower the total energy), the earlier the memory of the initial conditions is lost. Moreover, an influence of integration step sizes (i.e., time increments Δt) on numerical irreversibility is examined. As a result, even a small time increment could not improve reversibility of the present self-gravitating system, although the small time increment reduces global errors in total energy.

Key words: Self-gravitating system, Irreversibility, Round-off errors, N-body simulation
PACS: 04.40.-b, 05.70.Ln, 05.40.Ca, 02.70.Ns, 05.45.Pq

1 Introduction

N-body systems interacting with 'long-range potentials' exhibit several peculiar features, such as negative specific heat, violent relaxation, and non-

Email addresses: komatsu@t.kanazawa-u.ac.jp (Nobuyoshi Komatsu), skimura@t.kanazawa-u.ac.jp (Shigeo Kimura).

equilibrium nonextensive statistical mechanics [1–9]. Accordingly, investigation of these features has resulted in a lot of literature on astrophysically-motivated studies of temporal evolutions of self-gravitating systems (see e.g., Refs. [10–12] and references therein). In those studies, numerical simulations play an important role in investigating N-body systems, because we cannot solve such an N-body problem analytically. However, the numerical simulation inherently cannot avoid round-off errors, since floating-point real number arithmetic is employed. The influence of round-off errors becomes a serious problem, when we consider a system based on time-reversible laws, such as Newton's second law. This is because, even in the time-reversible system, numerical irreversibility arises from round-off errors.

In order to describe numerical irreversibility appearing in N-body simulations, we first review the work by Orban and Bellemans [13]. Their work is a good example from which to obtain a good understanding of numerical irreversibility in the simulation, although they investigated a *short-range* interacting system. Orban and Bellemans simulated the Loschmidt reversibility paradox on time-reversible dynamics, by using a hard-disk molecular dynamics (MD) method. In their simulation, a system of interactive molecules started from a non-equilibrium state, in order to observe the evolution of Boltzmann's H-function, $\mathrm{H}(t)= \int f(\mathbf{v}) \ln f(\mathbf{v}) d\mathbf{v}$, where $f(\mathbf{v})$ is a probability distribution for the particle velocity $\mathbf{v}$ at time t [14,15]. They confirmed that, during a certain time interval $0 \leq t \leq t_{\mathrm{rev}}$, the value of $\mathrm{H}(t)$ decreased with time t and approached the equilibrium state, in accordance with the Boltzmann's hypothesis. They then suddenly reversed all velocities of the molecules at time $t = t_{\mathrm{rev}}$, forcing the system to return to the initial nonequilibrium state. If the system is reversible, we can expect the value of $\mathrm{H}(t)$ to return to $\mathrm{H}(0)$ exactly. However, they found that the value of $\mathrm{H}(t)$ tended to return to the initial one but *not exactly*, i.e., numerical irreversibility due to round-off errors appeared in their simulation.

In chaotic and unstable systems such as the above N-body one, small noise has a significant influence on trajectories of all particles, since a small disturbance grows exponentially with time. Accordingly, the stability of N-body systems, which Krylov suggested [16], has been extensively studied; in particular, N-body systems interacting with 'short-range potentials' have been examined by using MD methods [17–22]. Nevertheless, since the standard MD simulation was not able to avoid round-off errors, the influence of round-off errors or irreversibility has not been investigated quantitatively [23–25], except for a few simple models [26–30]. Recently, however, in order to study numerical irreversibility in N-body systems, the present author [14,15,31] investigated systems interacting with 'short-range potentials', by means of a time-reversible MD method, i.e., a bit-reversible algorithm [32]. It was demonstrated that numerical irreversibility due to round-off errors correlated with the process of relaxation and the magnitude of the noise, and that the irreversibility propa-

gated through collisions between particles.

On the contrary, as for an N-body system interacting with 'long-range potentials', R.H. Miller [33–35] examined irreversibility in small stellar dynamical systems and showed that numerical errors grew exponentially with time. Since then, Lecar [36], Gurzadyan *et al.* [37], Kandrup [38,39], Goodman *et al.* [40] and many other researchers have investigated instability of self-gravitating systems [41–57]. For example, a relationship between the time scale for mixing and the number of particles N was evaluated and discussed in detail [37–40]. However, most of those previous studies examined only the instability of the system. Therefore, the irreversibility appearing in the self-gravitating N-body system has not yet been clarified, from the viewpoint of time-reversible dynamics. (For instance, in a typical star-rich cluster with a million stars, each star feels enough of the granularity of the gravitational field of the other stars that the consequent perturbations lead to a total loss of memory of the initial conditions of its orbit [11]. However, in the N-body simulations, numerical fluctuations due to round-off errors could behave as if they were the physical perturbations.)

In this context, in order to acquire a deeper understanding of the N-body simulation, we will investigate numerical irreversibility appearing in N-body systems with long-range interactions [58]. In the present paper, to examine a fundamental characteristic of the numerical irreversibility, we consider a self-gravitating N-body system enclosed in a spherical container with a reflecting wall [2,5,59–64]. In particular, we will investigate not only the influence of integration step sizes (i.e., time increments Δt), but also the influence of energy on the numerical irreversibility. This is because, in a short-range interacting system, the behavior of the irreversibility depends on the energy of the system [14]. That is, through this study, we investigate numerical irreversibility in self-gravitating systems and will attempt to bridge the gap between the short-range interacting system and the long-range interacting one. So far, the long-range interacting system such as the self-gravitating one has only been examined separately from the short-range interacting one.

The present paper is organized as follows. In Section 2, we give a brief review of MD techniques used for simulating a self-gravitating system enclosed in a spherical container with a reflecting wall. In Section 3, the initial conditions for the simulation are defined, and the time-reversal operation is described. In this section, we also describe several parameters which make a non-equilibrium behavior visible. In Section 4, the simulation results are presented. We first give an overview of the relaxation process, through a typical simulation result. Then, numerical irreversibility appearing in the system with various energy states is investigated and discussed. Moreover, the influence of the integration step size (i.e., the time increment Δt) on numerical irreversibility is examined as well. Finally, some conclusions are given.

2 Numerical methods

In order to simulate N-body systems with long-range interactions, we consider a typical problem which is known as the Antonov problem [1]. This is because it is the most fundamental one and has been extensively investigated in detail [2,5], especially by numerical simulations [59–64]. For simulating the Antonov problem, we consider a system consisting of N point-particles enclosed in a spherical container of radius R with reflecting (adiabatic) walls, as shown in Fig. 1. Accordingly, the present simulation is carried out under a restriction of constant energy, i.e., the microcanonical ensemble.

To simulate this system, we integrate the set of classical equations of motion for the particles interacting through the Plummer softened potential or an attractive soft Coulomb potential [61–64]. The Plummer softened potential is given by,

$$\Phi = -\frac{1}{\sqrt{r^2 + r_0^2}}, \tag{1}$$

where r and r_0 represent the distance between particles, and the soft core radius, respectively. In order to keep generality of the system, we set units as G=R=m=1, where G and m are the gravitational constant and the mass of a point-particle, respectively. The total energy E of the system is defined as,

$$E = E_{\rm KE} + E_{\rm PE} = \sum_{i}^{N} \frac{v_i^2}{2} - \sum_{i<j}^{N} \frac{1}{\sqrt{r_{ij}^2 + r_0^2}}, \tag{2}$$

where $E_{\rm KE}$, $E_{\rm PE}$ and v_i represent kinetic energy, potential energy and speed of the *i-th* particle, respectively. In order to use the traditional convention for self-gravitating systems, we define the total rescaled energy ε as,

$$\varepsilon = \varepsilon_{\rm KE} + \varepsilon_{\rm PE} = E\frac{R}{N^2}. \tag{3}$$

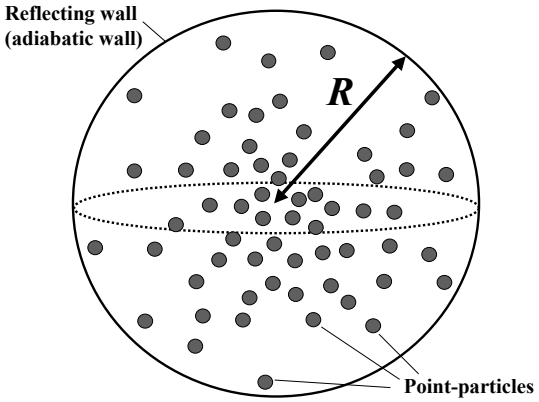

Fig. 1. Setup for the Antonov problem.

In the present study, $\sqrt{R^3/N}$ is chosen with the unit of time, which is calculated from both the unit of length R and the unit of velocity $\sqrt{N/R}$ [61].

In order to investigate numerical irreversibility due to round-off errors, we should avoid any other irreversibility appearing in simulations. That is, the scheme of the algorithm for the present simulation must be time-reversible. For this purpose, the set of equations of motion is integrated by using Verlet's algorithm (i.e., the leapfrog algorithm);

$$\frac{\partial^2 x_i}{\partial t^2}(\Delta t)^2 = x_i(t+\Delta t) - 2x_i(t) + x_i(t-\Delta t) = \sum_j f_{ij}(t)\,(\Delta t)^2, \qquad (4)$$

where $f_{ij}(t)$ is a partial force from the *j-th* particle on the *i-th* particle, located at position x_i at time t. It should be noted that, through the present simulations, all interparticle forces are calculated directly at each time step Δt, in order to avoid irreversibility due to the simulation procedure. For simulating the self-gravitating system, a double precision floating point real number is employed. Nevertheless, we can expect that exact time-reversibility of the simulation is violated due to round-off errors, i.e., numerical irreversibility will appear in the simulation [14,15,32].

As discussed in Refs. [37–40], the time scale for mixing depends on the number of point-particles N. However, in the present simulation, we focus on a fundamental characteristic of numerical irreversibility. Therefore, we consider a small system consisting of $N = 250$ point-particles in a spherical container of radius $R = 1$ [61]. In order to keep the total energy variation within 0.01% of its initial value, the time increment Δt is set to be 10^{-5}. (Note that, in Section 4.2, Δt is varied ranging from 10^{-4} to 10^{-6}, in order to study an influence of the time increment.) The soft core radius r_0 in Eq. 1 is fixed, that is, r_0/R is set to be 5×10^{-3}, for simulating self-gravitating systems properly. This is because a variation in the soft core radius has an influence on the stability of systems [43–47,51]. (For example, as r_0 is increased, the instability of the system or the Lyapunov exponent could decrease [45,51].) In the spherical container, to mimic the reflecting wall or the adiabatic wall, radial components of the velocity are reversed if the particle reaches the reflecting wall [63,64].

According to the numerical study by Ispolatov *et al.* [61], collapse and explosion energies for the present system are $\varepsilon_{coll} \approx -0.339$ and $\varepsilon_{expl} \approx 0.267$, respectively, since the soft core radius r_0 is set to be $5\times10^{-3}R$ in the simulation [65]. This means, if the total rescaled energy ε of the uniform state becomes lower than ε_{coll}, the system should undergo a collapse to a core-halo state. On the other hand, if the energy of the core-halo state becomes higher than ε_{expl}, the system should undergo an explosion. When the energy of the system is between ε_{coll} and ε_{expl}, the system should be in a stable or metastable state.

In the self-gravitating system, two time scales are typically considered: the first one is the crossing time τ_c corresponding to the free-fall time, and the second one is the relaxation time τ_r which is driven by the two-body encounter. For example, in our units, we can evaluate them as follows [4,63];

$$\tau_c \approx \sqrt{G\rho} = \sqrt{\rho}, \tag{5}$$

$$\tau_r \approx 0.1\tau_c \frac{N}{\ln N}, \tag{6}$$

where ρ represents the density of the system. Accordingly, in our units, the crossing and relaxation times of the present system become $\tau_c \approx 0.1$ and $\tau_r \approx 0.6$, respectively. That is, unlike astrophysically motivated studies, the order of the relaxation time is the same as that of the crossing time, because we consider a small N-body system.

3 Initial conditions and parameters for simulations

In order to simulate a time evolution of systems, the system is initially set to be in a highly non-equilibrium state. For this purpose, the initial velocity distribution is assumed to be one of a non-equilibrium state. Accordingly, for an initial setup, all the particles are set to have a velocity equal in $|\mathbf{v}_0|$ but with a random direction. Thereafter, in order to keep the total momentum and the total angular momentum as 0, the velocities of the particles are slightly modified, taking into account the subsequent density profile.

On the other hand, all the particles are initially distributed randomly in the spherical container, based on a spherically symmetric density profile. For this purpose, we set the initial density profile as follows: (1) The radial density profile is initially assumed to be a certain quasi-equilibrium one. In the present study, the initial density profile was set to be a quasi-equilibrium one for $\varepsilon \approx -0.3$, which was cited in Ispolatov *et al.* [61]. (2) In order to distribute the particles in the spherical container of radius $R = 1$, the container is first divided into 10 spherical shells in the radial direction r, where the distance between each inner outer shell is set to be $\Delta r = 0.1$. For example, the region of $0.9 < r < 1.0$ is the outermost shell. (3) Based on the radial density profile described in (1), the particles are distributed randomly in the spherical shells, taking into account a spherically symmetric profile.

According to these operations, the initial potential energies for the present simulations were set to be $\varepsilon_{\rm PE0} = -1.131 \pm 0.020$, where the error indicates a 68% confidence level in terms of the normal error distribution, by using the average over 100 simulations each with an identically-prepared initial setup. In other words, the initial density profiles and initial potential energies are

Table 1
Technical details for the initial setup.

$\varepsilon_{\rm target}$	ε	$\varepsilon_{\rm KE0}$	$\varepsilon_{\rm PE0}$
-0.7	-0.700 ± 0.021	0.431 ± 0.002	-1.131 ± 0.020
-0.3	-0.296 ± 0.021	0.835 ± 0.004	-1.131 ± 0.020
0.2	0.204 ± 0.021	1.335 ± 0.006	-1.131 ± 0.020
0.7	0.700 ± 0.022	1.831 ± 0.008	-1.131 ± 0.020

The target total rescaled energy is represented by $\varepsilon_{\rm target}$. The errors indicate a 68% confidence level in terms of the normal error distribution. Although the magnitude of the errors of the total rescaled energy depends on that of the initial potential energy, we have confirmed that these errors do not influence our main results. In this table, through each simulation, the total energy variation is below 0.01% of its initial value, and the time increment Δt is set to be 10^{-5}.

fixed. It is well-known that, under identically-prepared initial conditions, each simulation result is different from the others due to statistical fluctuations. However, we have confirmed that averaging over approximately 100 simulations is sufficient to see an averaged behavior. Therefore, all the results are averaged over 100 simulations with identically-prepared initial setups [66]. In this study, we investigate the averaged behavior of the system. Note that the initial potential energies are a little smaller than $\varepsilon_{\rm PE}^{\rm MF} = -0.944$, which is obtained from the Mean Field theory for $\varepsilon = -0.3$ [61]. However, we have confirmed that our main results in the present study are not influenced much by the initial density profiles. In order to examine the influence of energy, the total rescaled energy ε is varied, ranging from -0.7 to 0.7, under a restriction of constant initial potential energy. Those details for the initial setup are summarized in Table 1.

Now, to study numerical irreversibility due to round-off errors, we consider a typical problem which includes a time-reversal operation [14,15]. The system is initially in a highly non-equilibrium state. During the time evolution of the system, the time-reversal operation is applied at a certain time: i.e., all the particles reverse their velocities instantaneously at a certain time $t_{\rm rev}$. Therefore, the system evolves reversibly from then and, if the system is reversible, the initial state should appear again at $2t_{\rm rev}$. However, if the system contains any irreversibility, such as the numerical irreversibility, the initial state appears only incompletely or doesn't appear.

In the present study, for observing an overview of the non-equilibrium behavior, we define a ratio of velocity moments [61], vm(t), as

$$\mathrm{vm(t)} = \frac{< \mathbf{v}(\mathrm{t})^2 >^2}{< \mathbf{v}(\mathrm{t})^4 >}, \tag{7}$$

where $< X >$ represents a mean for X at time t [67]. We can expect that, even in the system with long-range interactions, the ratio of velocity moments de-

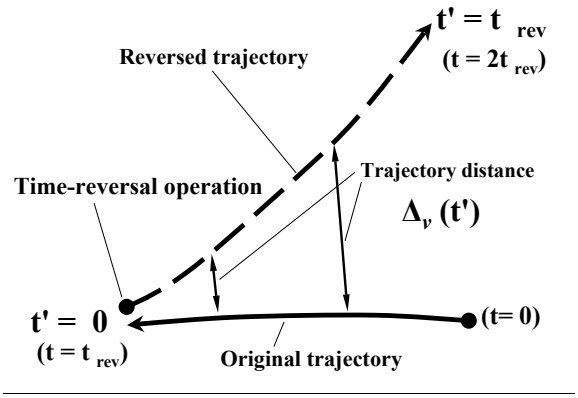

Fig. 2. Sketch of trajectory distance. The origin of t' is the time $t_{\rm rev}$ of the time-reversal operation.

creases from the initial value vm_0 towards a specific value $\mathrm{vm}_{\rm MB}$ corresponding to the Maxwell-Boltzmann velocity distribution. In fact, we have confirmed that, through the simulations, the ratio of velocity moments is quite consistent with the non-equilibrium behavior in the present system [68]. In the following, for simplicity, the ratio of velocity moments is normalized as

$$\mathrm{VM(t)} = \frac{\mathrm{vm(t)} - \mathrm{vm}_{\rm MB}}{\mathrm{vm}_0 - \mathrm{vm}_{\rm MB}}. \tag{8}$$

Accordingly, the normalized ratio of velocity moments VM(t) can be varied between 1 and 0, where 1 and 0 represents the initial value and the specific value corresponding to the Maxwell-Boltzmann velocity distribution, respectively.

It is well-known that the irreversible process and the stability of the system are closely related. Therefore, as shown in Fig. 2, we investigate a distance between two nearby trajectories, i.e., an original trajectory and a reversed one, through the time-reversible simulation [14]. The original trajectory is taken as the trajectory *before* the time-reversal operation, i.e., from $t = 0$ to $t = t_{\rm rev}$. On the other hand, the reversed trajectory is taken as the trajectory *after* the time-reversal operation, i.e., from $t = t_{\rm rev}$ to $t = 2t_{\rm rev}$. We can expect that, due to both round-off errors and instability of the system, the distance between two nearby trajectories increases with time. Note that, in this study, we consider a trajectory distance in (velocity) *speed* space [69]. The trajectory distance is given by,

$$\Delta_v(t') = \frac{\sqrt{\frac{1}{N}\sum_{i=1}^{N}(v_i^{(\rm original)} - v_i^{(\rm reverse)})^2}}{< v(0) >}, \tag{9}$$

where $v_i^{(\rm original)}$ and $v_i^{(\rm reverse)}$ are speed of the i-th particle at time t' for the

original trajectory and that for the reversed trajectory, respectively. It should be noted that the origin of t' is the time $t_{\rm rev}$ of the time-reversal operation, as shown in Fig. 2. That is, $< v(0) >$ represents the averaged speed at the time of the time-reversal operation, t'=0. We have confirmed that time evolutions of the trajectory distance defined here are consistent with the nonequilibrium behavior of the present system.

In the following, we mainly employ the trajectory distance at the final time $t' = t_{\rm rev}$, corresponding to $t = 2t_{\rm rev}$. The final trajectory distance is given by

$$\Delta_{v{\rm f}} \equiv \Delta_v(t' = t_{\rm rev}) = \left. \frac{\sqrt{\frac{1}{N}\sum_{i=1}^{N} (v_i^{(\rm original)} - v_i^{(\rm reverse)})^2}}{< v(0) >} \right|_{t'=t_{\rm rev}}. \tag{10}$$

In other words, the final trajectory distance $\Delta_{v{\rm f}}$ represents the trajectory distance between the original trajectory at the initial time $t = 0$ and the reversed one at the final time $t = 2t_{\rm rev}$.

4 Results

4.1 Effects of the total rescaled energy ε

By means of the MD simulation, we can now study numerical irreversibility in the self-gravitating system. Before proceeding further, however, it is appropriate to describe the relaxation process commonly observed in the present simulation. To this end, we first observe time evolutions of density, without the time-reversal operation. As a typical result, time evolutions of the shell-averaged density for $\varepsilon = -0.3$ are shown in Fig. 3. In this figure, for instance, the curve with '$r = 0.05$' represents the shell-averaged density between $r = 0.00$ and $r = 0.10$, where $r = 0.00$ represents the center of the spherical container shown in Fig. 1.

As shown in Fig. 3, each shell-averaged density varies quickly within the crossing time $\tau_c \approx 0.1$, and thereafter the density seems to approach a certain quasi-steady state gradually. As mentioned previously, the initial density profile is set to be a certain quasi-equilibrium one, corresponding to $\varepsilon \approx -0.3$. Nevertheless, since initial velocity distributions are in one of non-equilibrium states, the density profiles vary quickly, and gradually return to a quasi steady state for $\varepsilon = -0.3$. (Note that we observe an early stage of the relaxation process.) Next, we will focus on a peak of each curve, as designated by a dotted line with the arrow in Fig. 3. As a result, we can confirm that the peak of density propagates outward; i.e., from the inner region ($r = 0.05$) to the outer region ($r = 0.95$).

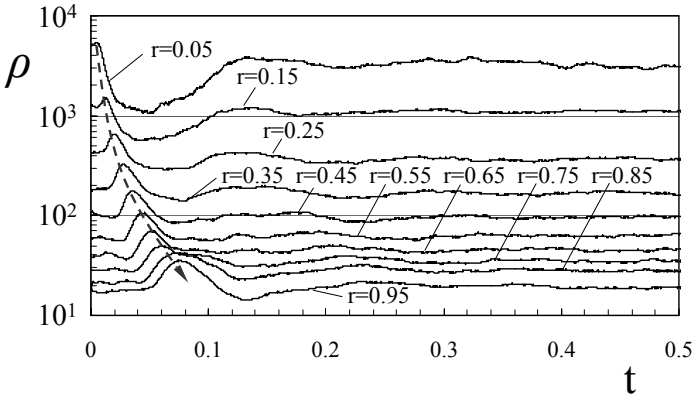

Fig. 3. Time evolutions of shell-averaged density for each shell, for $\varepsilon = -0.3$, without the time-reversal operation. Here, the r value is the mid-point radius within the shell (see the text).

Now, to observe numerical irreversibility in the present self-gravitating system, we will investigate time evolutions of normalized ratio of velocity moments, through the time-reversal operation. For this purpose, time evolutions of VM for $\varepsilon = -0.3$ are shown in Fig. 4. In this figure, the time-reversal operation is executed at the times designated by a, b, c, d and e; i.e., $t = t_{\rm rev} = 0.1, 0.2, 0.3, 0.4, 0.5$, respectively. As shown in Fig. 4, each VM decreases rapidly within the crossing time $\tau_c \approx 0.1$, and it gradually approaches a certain value before the times of the time-reversal operation $t_{\rm rev}$. These results are quite consistent with the relaxation process shown in Fig. 3. However, before $t_{\rm rev}$, the value of VM oscillates slightly because of the influence of the spherical reflecting wall, etc., and the value doesn't become 0. This means the velocity distribution is not completely the Maxwell-Boltzmann one. (From a dynamical or a statistical viewpoint, B.N. Miller *et al.* have carefully investigated a similar relaxation process in *one*-dimensional self-gravitating systems, through a velocity distribution, a time correlation function, etc. [52–57].)

After the times of the time-reversal operation $t_{\rm rev}$, in any case, VM doesn't go back to the initial state completely at $2t_{\rm rev}$; i.e., numerical irreversibility appears in the present simulation. According to Refs. [14,15], in order to measure these results quantitatively, a recovery rate of VM is newly-defined by

$$R_R \equiv \frac{\mathrm{VM}(2\mathrm{t_{rev}}) - \mathrm{VM}(\mathrm{t_{rev}})}{\mathrm{VM}(0) - \mathrm{VM}(\mathrm{t_{rev}})}. \tag{11}$$

The recovery rate R_R is a measure for the loss of reversibility in the system: that is, the smaller the recovery rate is, the more irreversible the system is.

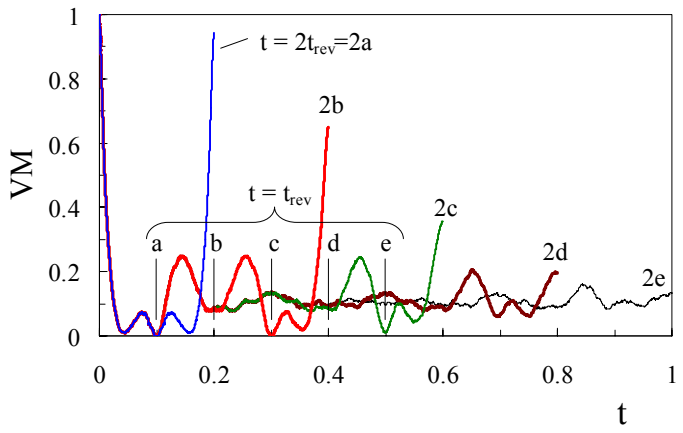

Fig. 4. (Color online) Time evolution of normalized ratio of velocity moments VM ($\varepsilon = -0.3$).

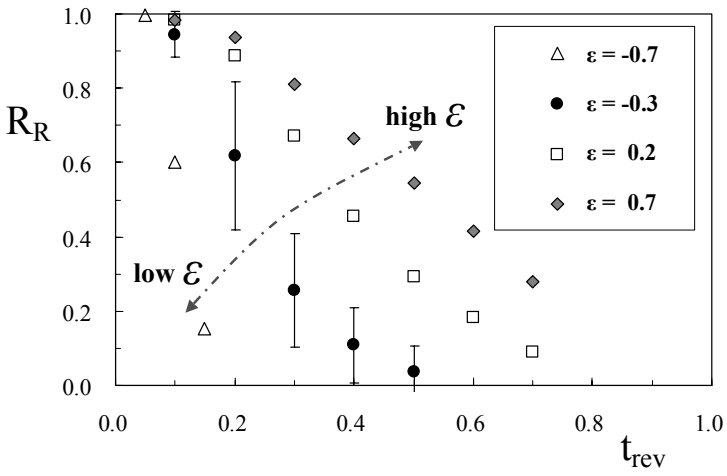

Fig. 5. Recovery rate R_R for various rescaled energies ε. The total rescaled energy is varied ranging from -0.7 to 0.7. Note that, in order to avoid confusion, the error bars for $\varepsilon = -0.3$ are shown as the typical ones. The error bars indicate the reliability of 68% confidence level in terms of the normal error distribution.

Using the recovery rate R_R, the results shown in Fig. 4 are re-plotted as closed-circles (•) in Fig. 5. As shown in Fig. 5, we can confirm that the recovery rate for $\varepsilon = -0.3$ becomes worse with increasing $t_{\rm rev}$. This result is consistent with the system with short-range interactions [13–15].

Next, we examine the influence of the total rescaled energy on the recovery rate R_R. For this purpose, Fig. 5 also depicts the results for various total rescaled energies, ranging from $\varepsilon = -0.7$ to $\varepsilon = 0.7$. As shown in Fig. 5, the

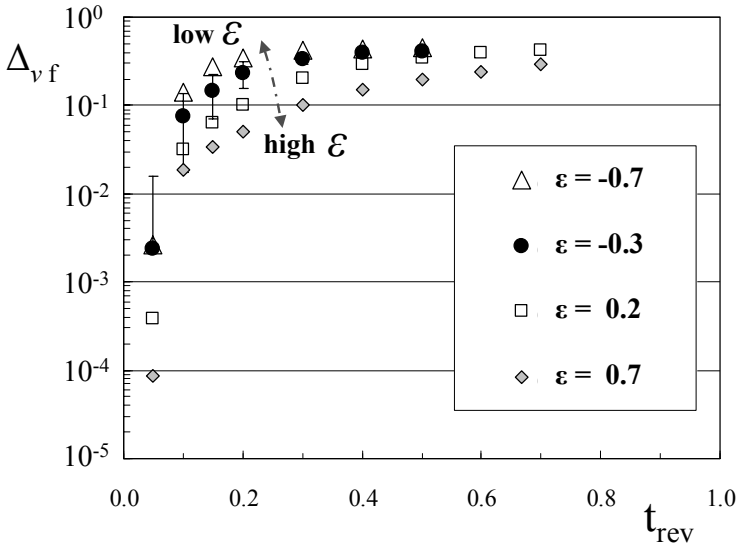

Fig. 6. Final trajectory distance Δ_{vf} for various rescaled energies ε. In order to avoid confusion, the error bars for $\varepsilon = -0.3$ are shown as the typical ones. The error bars for $\varepsilon = -0.3$ indicate the reliability of 68% confidence level in terms of the normal error distribution, by means of approximately 100 simulations.

irreversibility prevails rapidly with decreasing the total rescaled energy ε. As a matter of fact, as shown in Table 1, low total rescaled energy corresponds to low initial kinetic energy, since initial potential energy is fixed in the present study. Therefore, we can translate the result as follows. The lower the total rescaled energy is or the lower the initial kinetic energy is, the faster the influence of round-off errors prevails. Note that this characteristic is in contrast to that in the system interacting with the repulsive Lennard-Jones potential [14]. In that system, numerical irreversibility prevails rapidly with *increasing* initial kinetic energy, since numerical fluctuation propagates through collisions between particles.

Now, in order to examine this irreversible behavior from another viewpoint, we will investigate the final trajectory distance defined by Eq. 10. Figure 6 shows the final trajectory distance Δ_{vf}, for various total rescaled energies. As we expected, the final trajectory distance increases with increasing $t_{\rm rev}$. Moreover, the final trajectory distance increases with decreasing ε. Accordingly, these results are consistent with the ones obtained from the recovery rate R_R shown in Fig. 5. Through the simulations, we can confirm that not only the recovery rate but also the final trajectory distance is able to measure the irreversibility of the system.

As shown in Fig. 5 and 6, numerical irreversibility prevails rapidly with decreasing the total rescaled energy. In order to illustrate this, the following discussion based on a phase diagram of the system will be useful. In the present self-gravitating system, collapse and explosion energies are $\varepsilon_{coll} \approx -0.339$ and

$\varepsilon_{expl} \approx 0.267$, respectively. Accordingly, we can expect the following: (1) The systems for ε=0.7 and 0.2 could be in the relatively uniform state, (2) As for ε=$-$0.3, a density contrast between the inner and outer regions could be lower than that of a core-halo state, (3) Since the system for ε=$-$0.7 should undergo a collapse to a core-halo state, density and velocity at the core could increase quickly. (In fact, we have confirmed that the above three guesses are quite consistent with our simulation results.) Therefore, as for ε=$-$0.7, an influence of round-off errors prevails rapidly because of these many high-speed particles in the core. Note that, although the small N-body system for ε=$-$0.3 could collapse after a finite lifetime of metastable states [61,70,71], our simulation time, $t \sim 1$, is sufficiently shorter than the present lifetime, which is approximately 300 in our units.

In order to observe the behavior of numerical irreversibility more clearly and universally, we consider a propagation-time of numerical irreversibility for the present self-gravitating system. For example, as for the system interacting with the repulsive Lennard-Jones potential, the behavior of the irreversibility appearing in the system correlates with the mean collision time [14]. Similarly, the behavior of the irreversibility appearing in the self-gravitating system may correlate with the propagation-time of numerical irreversibility $\tau_{\rm p}$. To this aim, we define $\tau_{\rm p}$ as

$$\tau_{\rm p} \equiv t_{\rm VM=0.75}, \tag{12}$$

where $t_{\rm VM=0.75}$ represents the time required for VM = 0.75. Therefore, the propagation-time defined here depends on the above value, which is arbitrarily assigned. However, we have confirmed that our main result is qualitatively universal, even if the value is set to be other ones, e.g., $t_{\rm VM=0.80}$. Moreover, in the present study, the propagation-time $\tau_{\rm p}$ is nearly proportional to the initial kinetic energy $\varepsilon_{\rm KE0}$ or the total rescaled energy ε.

Using the propagation-time $\tau_{\rm p}$, we will investigate the behavior of numerical irreversibility shown in Fig. 5 and 6. To this aim, we first re-plot the recovery rate R_R against $t_{\rm rev}/\tau_{\rm p}$, as shown in Fig. 7. In this figure, to observe the behavior of numerical irreversibility more universally, the time of the time-reversal operation $t_{\rm rev}$ is divided by the propagation-time $\tau_{\rm p}$; i.e., the horizontal axis represents the time normalized by $\tau_{\rm p}$. As mentioned previously, in this study, $\tau_{\rm p}$ is nearly proportional to $\varepsilon_{\rm KE0}$ or ε. As a result, as shown in Fig. 7, all the results for various energies agree well with each other. Similarly, as shown in Fig. 8, when we re-plot the final trajectory distance Δ_{vf} against $t_{\rm rev}/\tau_{\rm p}$, all the results agree with each other. (It should be noted that, in Fig. 7 and 8, the results for ε=$-$0.7 are slightly different from the others.) This means that, in the present self-gravitating system, the behavior of numerical irreversibility depends on the propagation-time. Moreover, for $t_{\rm rev}/\tau_{\rm p} \gtrapprox 120$, the simulated trajectory completely forgets its initial conditions. This time should correlate with *the dynamical memory time* t_m suggested by Norman *et al.* [29], where t_m is related to both fluctuation of energy ΔE and K-entropy (or the Lyapunov

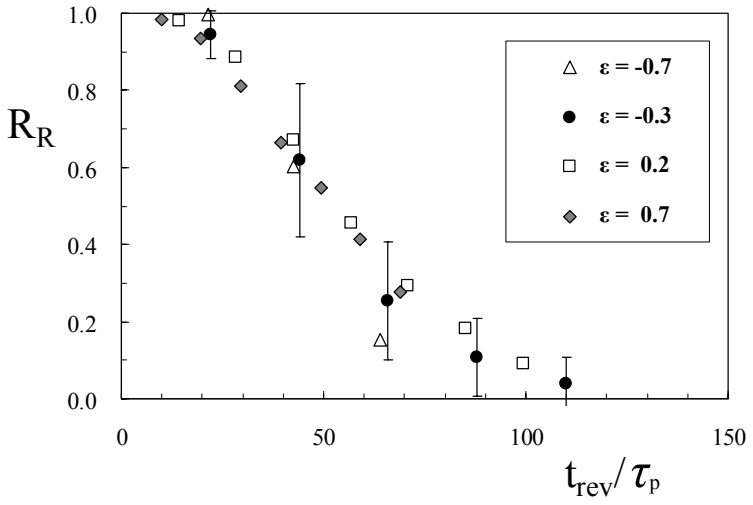

Fig. 7. Influence of the total rescaled energy on the recovery rate R_R. The results shown in Fig. 5 are re-plotted. In this figure, the elapsed time is normalized by the propagation-time $\tau_{\rm p}$. For the details, see the caption of Fig. 5.

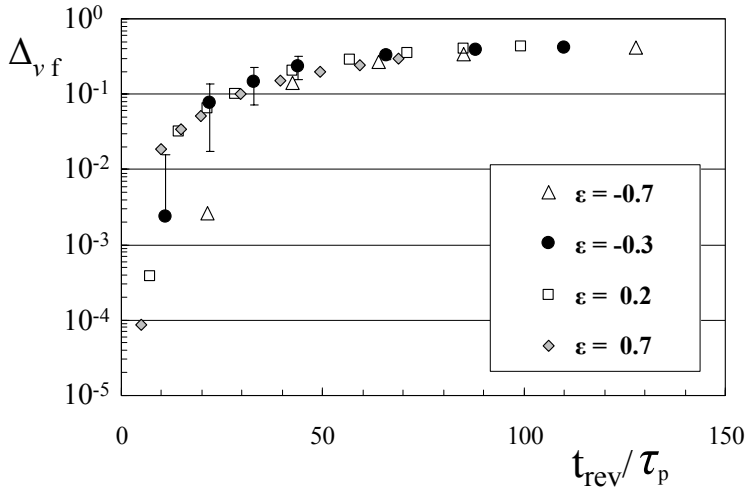

Fig. 8. Influence of the total rescaled energy on the final trajectory distance Δ_{vf}. The results shown in Fig. 6 are re-plotted against the time normalized by $\tau_{\rm p}$. For the details, see the caption of Fig. 6.

exponent). However, the propagation time and dynamical memory time are different from each other, in the sense that the former is nearly proportional to the total rescaled energy or the initial kinetic energy in the present study.

In this subsection, to examine an influence of the time increment, Δt is varied ranging from 10^{-4} to 10^{-6}, for $\varepsilon = -0.7$ and $t_{\rm rev}$=0.1. The other specifications are the same as those in Section 4.1. As a result, as shown in Fig. 9, the relative deviation of total energy $\Delta\varepsilon/\varepsilon$ (i.e., global error in total energy) decreases with decreasing Δt. Here $\Delta\varepsilon$ represents the standard deviation of the total rescaled energy, in terms of the normal error distribution. This result is well-known: e.g., see a textbook on molecular dynamics simulations [72] or Ref. [73].

On the other hand, as for the recovery rate R_R, the error bars for R_R are significantly large in the simulation (Note that this error represents statistical fluctuations.). However, it seems at least that a small time increment could not improve time-reversibility of the present self-gravitating system. Similarly, as for the final trajectory distance Δ_{vf}, it seems that Δ_{vf} is not influenced much by the time increment. This is an unexpected result, since we expected the small time increment could improve the reversibility of the system.

In order to investigate the influence of the time increment more clearly, we will examine time evolutions of the trajectory distance $\Delta_v(t')$. As shown in Fig. 10, the initial values of the trajectory distance are the common one at the first time step (i.e., at t' =1Δt), although the first times are different from each other. After the first time step, all the curves increase gradually with time ($t' \lessapprox 10^{-2}$),

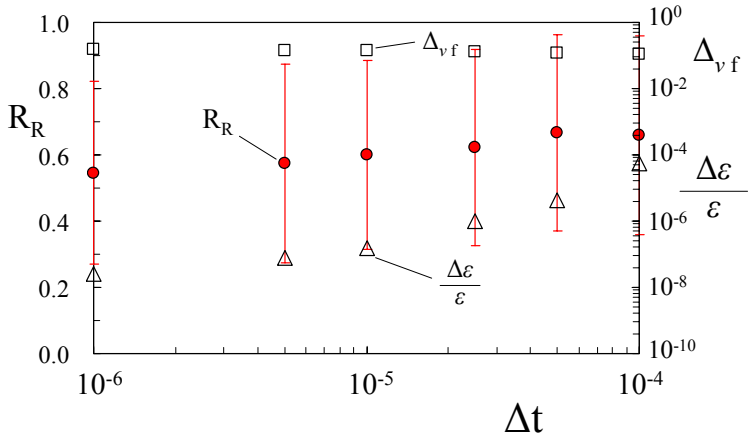

Fig. 9. (Color online) Influence of the time increment for $\varepsilon = -0.7$ and $t_{\rm rev}$=0.1. The closed circles, the open squares and the open triangles represent the recovery rate R_R, the final trajectory distance Δ_{vf} and the relative deviation of total energy $\Delta\varepsilon/\varepsilon$, respectively. In order to compute $\Delta\varepsilon/\varepsilon$, ε was output every 5.0×10^{-5} time step, through the simulations except for Δt=10^{-4}.

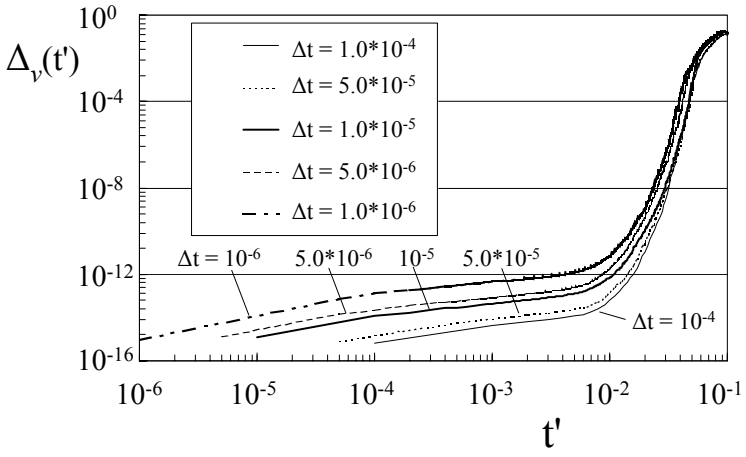

Fig. 10. Time evolutions of the trajectory distance $\Delta_v(t')$ with various time increments, for $\varepsilon = -0.7$ and $t_{\rm rev}$=0.1. The origin of t' is the time $t_{\rm rev}$ of the time-reversal operation. The horizontal axis, t', is indicated by a logarithmic axis, in order to observe a difference between the curves clearly. The trajectory distance was plotted every $10\Delta t$ steps.

and they increase exponentially ($10^{-2} \lessapprox t' \lessapprox 0.5 \times 10^{-1}$). Thereafter, the trajectory distance $\Delta_v(t')$ increases slowly and becomes saturated. Moreover, the slope of the curves, which corresponds to instability of the system, is comparable to each other. That is, after the first time step, the time evolutions of the trajectory distance are comparable to each other, since instability of the systems is almost equivalent. Therefore, the final trajectory distance shown in Fig. 9 is not influenced much by the time increment, even though the small time increment reduces the relative deviation of total energy.

5 Conclusions

It is well-known that, although numerical irreversibility due to round-off errors may behave as if it were a physical one, it is not a physical one. Therefore, in order to study such numerical irreversibility appearing in self-gravitating N-body systems, we investigated a closed spherical system consisting of N=250 particles, by means of molecular dynamics methods. In the present study, to examine the numerical irreversibility, a time-reversal operation was applied at a certain time during the evolution of the system. Through the present simulation, we demonstrated that the normalized ratio of velocity moments was consistent with an early stage of the relaxation process. We found that, under a restriction of constant initial potential energy, the numerical irreversibility prevailed rapidly with decreasing an initial kinetic energy or total

energy. In other words, the lower the initial kinetic energy or the lower the total energy, the earlier the memory of the initial conditions is lost. The behavior of numerical irreversibility depends on a propagation-time proposed in the present study. Moreover, we examined an influence of the time increment Δt on numerical irreversibility. As a result, the small time increment could not improve reversibility of the present self-gravitating system, even though it reduces global errors in total energy.

References

[1] V.A. Antonov, *in Dynamics of Globular Clusters*, edited by J. Goodman and P. Hut, IAU Symposium No. 113, (Reidel, Dordrecht, 1985); Vestn. Lening. Gos. Univ. 7 (1962) 135.

[2] D. Lynden-Bell, R. Wood, Mon. Not. R. Astron. Soc. 138 (1968) 495.

[3] A.P. Lightman, S.L. Shapiro, Rev. Mod. Phys. 50 (1978) 437.

[4] J. Binney, S. Tremaine, *Galactic Dynamics*, Princeton University Press, Princeton, 1987.

[5] T. Padmanabhan, Phys. Rep. 188 (1990) 285.

[6] D. Lynden-Bell, Physica A 263 (1999) 293.

[7] C. Tsallis, J. Stat. Phys. 52 (1988) 479.

[8] V. Latora, A. Rapisarda, C. Tsallis, Phys. Rev. E 64 (2001) 056134.

[9] S. Abe, A.K. Rajagopal, Phys. Lett. A 272 (2000) 341.

[10] S.J. Aarseth, *Gravitational N-Body Simulations: Tools and Algorithms*, Cambridge University press, Cambridge, 2003.

[11] D.C. Heggie, P. Hut, *The gravitational million-body problem*, Cambridge University press, Cambridge, 2003.

[12] H. Baumgardt, D.C. Heggie, P. Hut, J. Makino, Mon. Not. R. Astron. Soc. 341 (2003) 247.

[13] J. Orban, A. Bellemans, Phys. Lett. 24A (1967) 620.

[14] N. Komatsu, T. Abe, Physica D 195 (2004) 391.

[15] N. Komatsu, T. Abe, Comput. Phys. Commun. 171 (2005) 187.

[16] N.S. Krylov, *Works on the Foundations of Statistical Physics*, Princeton University Press, 1979.

[17] H.A. Posch, W.G. Hoover, Phys. Rev. A 38 (1988) 473.

[18] W.G. Hoover, Physica D 112 (1998) 225.

[19] W.G. Hoover, *Time reversibility, Computer simulation, and Chaos*, World Scientific Publishing Co., 1999.

[20] Ch. Dellago, H.A. Posch, Physica A 230 (1996) 364.

[21] Ch. Dellago, H.A. Posch, W.G. Hoover, Phys. Rev. E 53 (1996) 1485.

[22] I.V. Morozov, G.E. Norman, A.A. Valuev, Phys. Rev. E 63 (2001) 036405.

[23] K. Jansen, C. Liu, Nucl. Phys. B453 (1995) 375.

[24] R.G. Edwards, I. Horváth, A.D. Kennedy, Nucl. Phys. B484 (1997) 375.

[25] B.D. Todd, P.J. Daivis, J. Chem. Phys. 112 (2000) 40.

[26] N.J. Higham, SIAM J. Sci. Comput. 14 (1993) 783.

[27] W. Thirring, H.A. Posch, Phys. Rev. E 48 (1993) 4333.

[28] Ch. Dellago, W.G. Hoover, Phys. Rev. E 62 (2000) 6275.

[29] G.E. Norman, V.V. Stegailov, Comput. Phys. Comm. 147 (2002) 678.

[30] J. Kumicak, Phys. Lett. A 356 (2006) 397.

[31] N. Komatsu, T. Abe, Phys. Fluids 19 (2007) 056103.

[32] D. Levesque, L. Verlet, J. Stat. Phys. 72 (1993) 519.

[33] R.H. Miller, Astrophys. J. 140 (1964) 250.

[34] R.H. Miller, J. Comput. Phys. 2 (1967) 1.

[35] R.H. Miller, J. Comput. Phys. 8 (1971) 449.

[36] M. Lecar, Bull. Astron. 3 (1968) 91.

[37] V.G. Gurzadyan, G.K. Savvidy, Astron. Astrophys. 160 (1986) 203.

[38] H.E. Kandrup, Phys. Lett. A 140 (1989) 97.

[39] H.E. Kandrup, Physica A 169 (1990) 73.

[40] J. Goodman, D.C. Heggie, P. Hut, Astrophys. J. 415 (1993) 715.

[41] S.J. Aarseth, M. Lecar, Ann. Rev. Astron. Astrophys. 13 (1975) 1.

[42] M. Sakagami, N. Gouda, Mon. Not. R. Astron. Soc. 249 (1991) 241.

[43] Y. Suto, PASJ. 43 (1991) L9.

[44] H.E. Kandrup, H. Smith, Astrophys. J. 374 (1991) 255.

[45] H.E. Kandrup, H. Smith, D.E. Willmes, Astrophys. J. 399 (1992) 627.

[46] A.A. El-Zant, Astro. Astrophys. 326 (1997) 113.

[47] A.A. El-Zant, Astro. Astrophys. 331 (1998) 782.

[48] M. Cerruti-Sola, M. Pettini, Phys. Rev. E 51 (1995) 53.

[49] M. Hemsendorf, D. Merritt, Astrophys. J. 580 (2002) 606.

[50] D. Huber, D. Pfenniger, Astron. Astrophys. 386 (2002) 359.

[51] W. Hayes, Am. J. Phys. 72 (2004) 1251.

[52] H.L. Wright, B.N. Miller, W.E. Stein, Astrophys. Space Sci. 84 (1982) 421.

[53] H.L. Wright, B.N. Miller, Phys. Rev. A 29 (1984) 1411.

[54] C.J. Reidl, B.N. Miller, Astrophys. J. 318 (1987) 248.

[55] C.J. Reidl, B.N. Miller, Astrophys. J. 332 (1988) 619.

[56] B.N. Miller, C.J. Reidl, Astrophys. J. 348 (1990) 203.

[57] C.J. Reidl, B.N. Miller, Phys. Rev. A 46 (1992) 837.

[58] N. Komatsu, *et al.*, Proc. of Int. Conf. Comput. Method, ICCM2007, G4-11, pp.91, Hiroshima, JAPAN, 2007: The Eighteenth International Symposium on Transport Phenomena, ISTP18-83, pp.2031-2036, Daejeon, KOREA, 2007.

[59] H. Endoh, T. Fukushige, J. Makino, Publ. Astron. Soc. Japan 49 (1997) 345.

[60] A.A. El-Zant, Phys. Rev. E 58 (1998) 4152.

[61] I. Ispolatov, M. Karttunen, Phys. Rev. E. 68 (2003) 036117.

[62] A. Taruya, M. Sakagami, Physica A 307 (2002) 185.

[63] A. Taruya, M. Sakagami, Phys. Rev. Lett. 90 (2003) 181101.

[64] A. Taruya, M. Sakagami, Mon. Not. R. Astron. Soc. 364 (2005) 990.

[65] Although the explosion energy is sensitive to the soft core radius r_0, the collapse energy is not influenced much by r_0: For example, for $r_0 = 0$, the collapse energy is $\varepsilon_{coll} = -0.335$.

[66] In several cases, the results are averaged over approximately 100 simulations, at least more than 88 simulations.

[67] In general, to make a non-equilibrium behavior visible, Boltzmann's H-function or the Boltzmann-Gibbs entropy has been employed. However, in systems with long-range interactions, the H-function is not suitable for observing the non-equilibrium behavior, because the potential energy varies temporally. Moreover, in those systems, it is difficult to discuss the thermodynamics or the Boltzmann-Gibbs statistical mechanics in the standard formalism, due to the long-range interactions and to their nonadditivity, since the Newtonian potential is singular and has infinite range. Note that, for preparing the present initial density profile, we employ the result obtained from the mean field theory which assumes the Boltzmann-Gibbs entropy. This is because we consider a closed spherical system with a reflecting wall; i.e., the present system is confined in a finite volume.

[68] This doesn't mean the ratio of velocity moments is the most suitable for observing the non-equilibrium behavior.

[69] This is because, if a particle reaches a reflecting wall, the radial component of the velocity is suddenly reversed and the particle position is changed.

[70] J. Katz, I. Okamoto, Mon. Not. R. Astron. Soc. 317 (2000) 163.

[71] P.H. Chavanis, astro-ph/0404251v1.

[72] J.M. Haile, *Molecular dynamics simulation, :Elementary methods*, John Wiley & Sons, INC., 1997.

[73] A finite difference method, such as Verlet's algorithm, incurs two types of errors: truncation errors and round-off errors [72]. That is, global errors in total energy are composed of truncation errors and round-off errors. In the present simulation, the global errors are dominated by truncation errors and, therefore, the global errors decrease with decreasing Δt. However, for a smaller time increment, the global errors are dominated by round-off errors.